PREDICTION OF TIME-DEPENDENT SUBSIDENCE, TILT AND HORIZONTAL STRAIN OVER UPWARDS MIGRATED SALT SOLUTION CAVITIES

R.F. Bekendam[a], C. Oldenziel[b] & W.A. Paar[b]

[a]BGT, Meidoorn 93, 6226 WG Maastricht, The Netherlands
[b]Akzo-Nobel Chemicals bv, Minerals Department, Postbus 25, 7550 GC Hengelo (Ov), The Netherlands

Overmining of salt solution wells will generally give rise to migration of the cavity towards the surface due to progressive upward roof rock failure, a process denoted as stoping. The rock layers are sometimes overlain by a soil overburden of a large thickness relative to the diameter of the migrating cavity. If the stoping process is not arrested by bulking or arching and the cavity reaches the base of the soil units, significant subsidence at the surface will arise. In the Hengelo brine field, East Netherlands, five areas of trough subsidence developed due to gradual deflection of the soil overburden into the migrated cavity. Compaction of the about 200 m high debris chimney under the overburden load is responsible for further surface subsidence, which will proceed for a long time at a continuously decreasing rate.

The subsidence-time relationship proved to be well described by a log-normal function. Analysis of field data showed that the shape of the subsidence bowl is well defined by a Litwiniszyn-type influence function. Now it is possible to predict future ground movement at any surface point. If a set of field data is available for calibration, this empirical method can be applied in any comparable setting, providing a means to estimate damage to houses and other surface structures.

1. INTRODUCTION

Salt solution mining sometimes brings about trough subsidence or even sinkhole formation. These ground movements may only develop when the uppermost salt layers have been disappeared due to overmining. As a result of progressive upward roof failure the cavity migrates towards the surface. If this stoping process is not arrested by bulking or arching subsidence at the surface will result, normally many years after the creation of the cavity.

In the Hengelo area, East Netherlands, a near-horizontal, more or less continuous rock salt layer of about 50 m thickness is mined by Akzo-Nobel since 1933. The salt deposit of Upper Triassic age is situated at about 350 to 400 m depth and is overlain by mainly friable claystones. The Mesozoic rock layers do not continue up to the surface but are covered by about 100 m of clayey Tertiary and Quaternary soil units. If a cavity is capable of migrating up to the base of the clays, the ductile soil mass of a relatively low stiffness gradually subsides over the migrated opening and a subsidence bowl develops at an angle of draw of about 45° from the rock-soil interface [1]. Hence, due this soil overburden, surface subsidence normally evolves as a trough and not as a sinkhole. In this brine field five areas of trough subsidence and one sinkhole were formed over old wells, which date from the sixties or earlier. The subsidence troughs measure 150 to 300 m diameter and at present 1 to 3.5 m depth. The sinkhole of 35 m diameter and 4.5 m depth is attributed for an important part to its location near a tectonic fault. In a surface subsidence vs. time plot (Figs. 1-2) three phases may be distinguished [2]. Each phase corresponds to different events in the subsurface:

- phase I: convergence of a cavity which is situated completely within the salt formation. Surface subsidence is negligible (0.5 mm/year at most).
- phase II: in case of overmining, upward migration of the cavity through the friable roof rocks at rates from 5 to 15 m/year. This phase can be detected at the surface by a precursory, constant or slightly increasing subsidence rate of several mm per year.
- phase III: the soil mass subsides over the opening, if this arrives near the rock-soil interface (Fig. 3). A subsidence bowl develops, as described above. At the onset of this phase surface

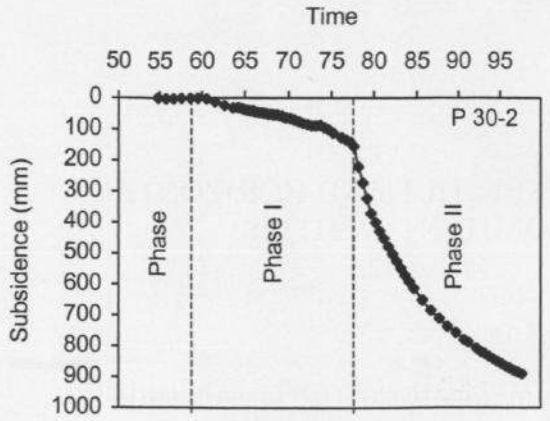

Figure 1. Subsidence vs. time (in years) at point 30-2.

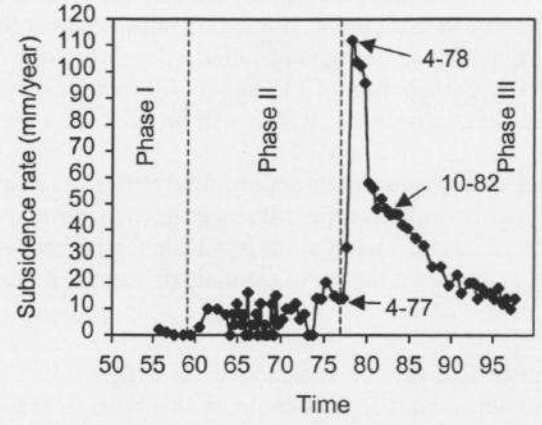

Figure 2. Subsidence rate as a function of time (in years) at point 30-2.

subsidence suddenly accelerates significantly, and then continuously decelerates.

Phase III subsidence proceeds for a long time, at least for tens of years, because compaction is involved of a generally more than 200 m high chimney of roof debris, which has been left by the migrated cavity. It is of interest to be able to predict the future development of this surface subsidence, tilt and strain. For example, one area of surface subsidence evolved in 1973 under the purification and vacuum plant. Periodically it is necessary to jack up purification tanks and to adjust foundations. An adequate prediction allows to refine long-term planning for preventive maintenance. It also provides the means to assess where new surface structures can be erected according to allowable values of components of ground movement.

Based on an analysis of regular measurements of subsidence and horizontal displacement, a curve-fitting method was developed which gives an accurate prognosis of further subsidence developments at a given surface point. Additionally, the spatial distribution of subsidence data proved to be well described by influence functions. By combining these results, surface contour plots could be constructed which indicate subsidence, tilt and strain for a whole subsidence trough at a given time in the future.

2. RELATIONSHIP BETWEEN SUBSIDENCE AND TIME

Various mathematical functions were attempted to characterize phase III subsidence as a function of time. Plotting subsidence vs. the logarithm of time gave good results. In the same way creep deformation of rock [3,4] and soil [5] can often be described. This fitting method is commonly used as well in soil mechanics to describe compression of a sample during a consolidation test [5]. In fact phase III subsidence can be considered as a large-scale, complex consolidation experiment. The time-dependency of subsidence may be determined by time-dependent downward deflection of the soil overburden, dissipation of excess brine pressure in the debris column (primary compression) and creep deformation of the debris itself, for instance by slow adjustment of fragments to more stable arrangements (secondary compression). Additionally, the debris column is of such a height, that compression under its own weight must be considered as well. A quantitative analysis of these physical processes remains to be accomplished.

The fitting method is illustrated here for levelling point 30-2, which is located more or less in the centre of the subsidence area at wells 30 and 31. These wells were drilled in 1953 and became interconnected in 1957. Production ceased in 1964. After phase II subsidence at a constant to slightly increasing rate of about 7 mm/year on the average, phase III subsidence was detected in April 1977 (Figs. 1-2). Since April 1978 subsidence is decelerating continuously. Initially the subsidence vs. log time curve proved to be convex upwards for a few years, but appears as a straight line from then onwards until today (Fig. 4). A linear relationship

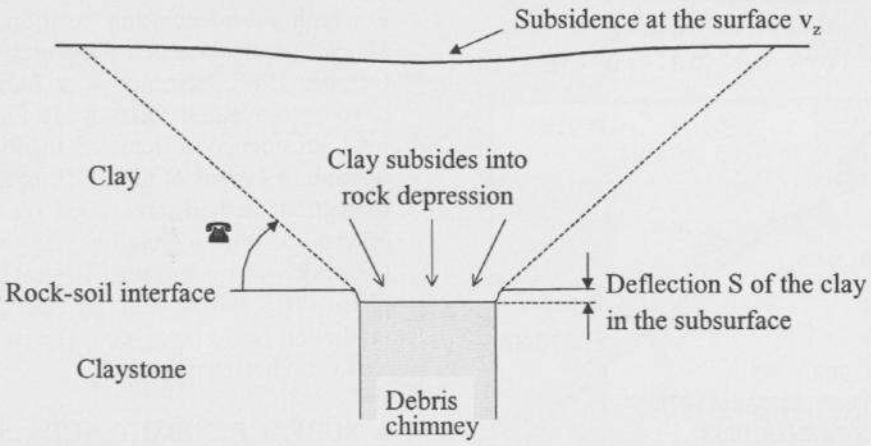

Figure 3. Development of Phase III trough subsidence.

only results if subsidence and time are reset to zero at the beginning of the decrease of the subsidence rate, which is here in April 1978. Therefore $\Delta v_{z,IIID} = v_{z,tot} - v_{z,IIID}$ and $\Delta t_{IIID} = t_{tot} - t_{IIID}$ are used as regression parameters. Here $v_{z,tot}$ and t_{tot} are total subsidence and time respectively, while $v_{z,IIID}$ and t_{IIID} signify respectively subsidence and time, since the first levelling measurement, at the onset of phase III deceleration. When t_{IIID} and $v_{z,IIID}$ are taken earlier or later, the curve becomes convex respectively concave upwards over its entire range.

Consider the situation in October 1986 when 13 data points, indicated by blacksymbols, are available to establish a trend for future phase III subsidence till 1997, not known at that time (Fig. 4). The question was how to separate the linear part, which serves as a basis of prediction of further subsidence, from the non-linear part, which should not be used for the regression line. Clearly not all data points, from October 1979 onwards, should be utilised. For a non-arbitrary separation of data points regression lines were tested for serial correlation in the residuals u_i, where

$$\Delta v_{z,IIID} = a + b \log \Delta t_{IIID} - u_i \qquad (1)$$

Here a is the Y-axis intercept and b is the slope of the regression line. For an adequate fit the residuals must be randomly distributed with a mean of zero. If the value of a residual depends on the value of the next one, then a systematic variation exists. For example serial correlation increases significantly if in the analysis data points are included well before October 1982. Serial correlation can be described by the Durbin and Watson [6] statistic:

$$DW = \Gamma (u_i - u_{i-1})^2 / \Gamma u_i^{\,2} \qquad (2)$$

The authors tabulated critical values for DW against n, the number of observations. If the observed DW exceeds dU, the so-called upper bounds, serial correlation can be excluded. Here the 95 % confidence level was used for the test. First all data points, from October 79 to October 86, were used for a linear regression, which was then subjected to the test for serial correlation. As additional criteria, the correlation coefficient R^2 should be at least 0.95 and the confidence level of the regression, using an F-test, should be at least 95 %. The regression was accepted when all three criteria are satisfied. If not, than the first observation pair, in this case that of October 1979, was omitted and the remaining data were fitted again. This procedure was repeated until the subsidence-time relationship fitted the criteria. In this case 6 data points had to be omitted, leaving 7 data points, from October 1982 till October 1986. An excellent fit was achieved with $R^2 = 0.999$ and a confidence level of nearly 100 % for a = -75 and b = 577. Subsidence and time are expressed in mm and years respectively. Since the regression also fits later measurements well (blank symbols in Fig. 4) it proved to be an adequate tool for subsidence prediction.

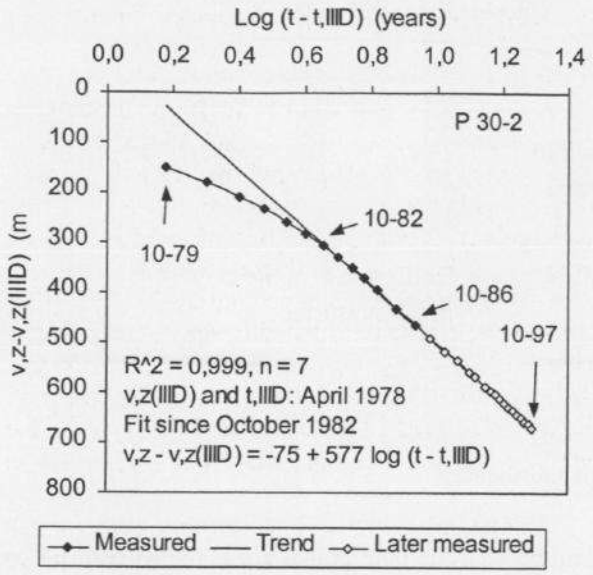

Figure. 4 Subsidence during phase III deceleration vs. log time(years) at point 30-2

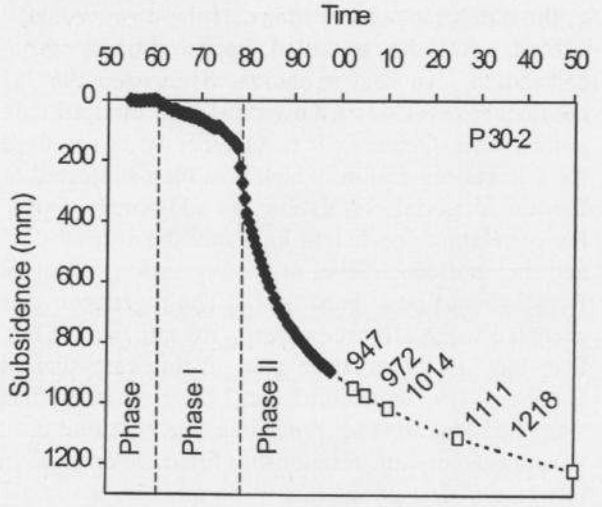

Figure 5. Subsidence prediction for point 30-2 by means of Eq. 3.

To predict subsidence for the next century, 24 data points from October 1982 till October 1997 were used. Now the following equation resulted:

$$\Delta v_{z,IIID} = -76 + 578 \log \Delta t_{IIID} \qquad (3)$$

For both subsidence-time relationships a and b are almost identical, which illustrates that prediction in October 1986, based on just 7 data points, would have been adequate already. In Fig. 5 the predicted total subsidence is depicted till 2050. Also for the remaining 4 areas of phase III trough subsidence the prediction method gave good results and the three criteria of the regression line were amply met. Generally within less than 10 years after the onset of phase III subsidence an adequate subsidence prediction could be given. The method also applies to tilt and horizontal strain.

3. SURFACE SUBSIDENCE AS A FUNCTION OF BOTH TIME AND LOCATION

The method described above accurately predicts subsidence for one individual surface point, but seems time-consuming if predictions are required for a whole subsidence trough. In that case the method should be applied to each surface point separately. Moreover, measuring points were not always installed over the whole subsidence area and at many of those points data have not been acquired during the entire subsidence period. Therefore an additional method was chosen in order to describe the spatial distribution of surface subsidence as well, on the basis of a limited number of data from one or more measuring profiles.

Consider the soil overburden which subsides, during compaction of the debris chimney, into the resulting rock depression, which depth S(t) is continuously increasing. The subsurface subsidence S(t) brings about a trough-like subsidence area at the surface, which is deepening concurrently but remains the same in shape. The subsidence trough is bounded by the angle of draw (, which is about 45° [1] for this soil mass (Fig. 3). The spatial distribution of surface subsidence, i.e. the shape of the trough, can be characterized by a function F(x,y). This function is independent of t and has as variables the coordinates x and y relative to the centre (x = y = 0) of the subsidence bowl. If S(t) and F(x,y) are both known, phase III surface subsidence can be determined at any point (x,y) and any time t according to the expression:

$$v_z(x,y,t) = F(x,y) * S(t) \qquad (4)$$

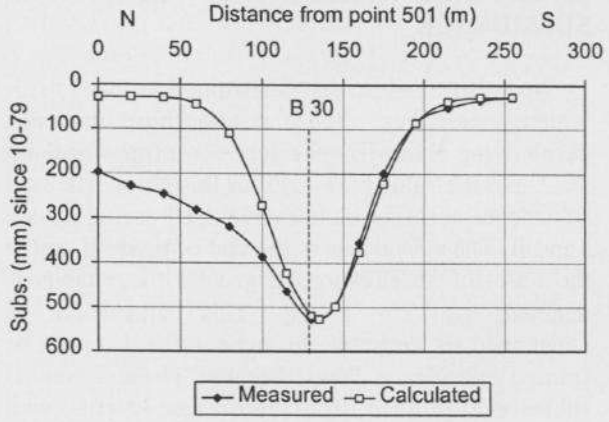

Figure 6. N-S subsidence profile at wells 30-31.

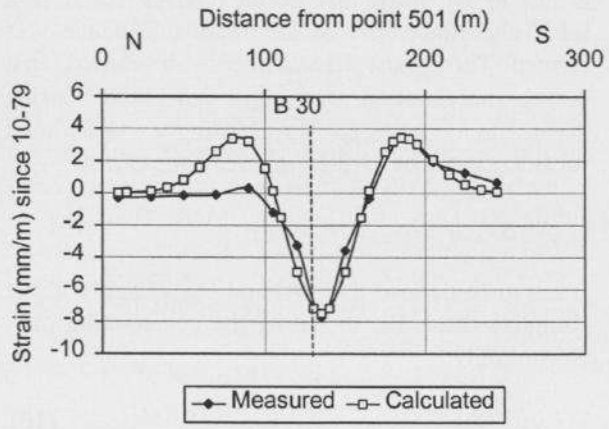

Figure 7. N-S horizontal strain profile at wells 30-31

4. SPATIAL DISTRIBUTION OF SURFACE SUBSIDENCE

Fig. 6 shows an N-S profile of the subsidence trough at wells 30 and 31, measured in April 1994. The profile applies to levelling since October 1979 and thus relates to more or less "pure"phase III subsidence. 3D high resolution reflection seismic data [7] revealed that the depression at the base of the soil mass is more or less circular, 1 to 3 m deep and approximately centred at well 30. The profile line runs about 15 m to the west of the centre of the trough. The northern part is affected by the deep subsidence bowl near wells 33-36. Therefore only the southern half of the profile is representative for subsidence due to the subsurface depression of wells 30-31. The corresponding strain profile is depicted in Fig. 7.

It was attempted to characterise the profiles by means of influence functions [8]. These empirically based functions not only give subsidence but also other components of ground movement at each surface point, irrespective of the shape of the underground opening. The method is based on the concept of the area of influence. This is a circular area at the level of the underground opening or depression, which is bounded by the angle of draw (Fig. 8). Only openings or depressions inside this area can affect the subsidence at a surface point P. Its so-called radius of influence R is equal to the product of depth h and the tangent of γ. Here R = h because $\gamma = 45°$.

An influence function k_z describes the very small amount of subsidence dv_z at a surface point P due to a certain infinitesimal element dA of the subsurface depression:

$$k_z = d\,v_z / d\,A \qquad (5)$$

It can be imagined that the contribution of elements to subsidence in point P decreases with increasing distance r from the centre of the area of influence. Now, using Carthesian coordinates, subsidence at point P is obtained by solving the double integral:

$$v_z = \iint_{x\,y} k_z(x, y)\,dx\,dy \qquad (6)$$

From the various influence functions which were applied the Litwiniszyn-type function with n = 4 proved to give the best results for all 5 subsidence bowls:

$$k_z = (n\,S / R^2) * \mathrm{Exp}\,[-nB\,(x^2 + y^2 / R^2)] \qquad (7)$$

In order to use Carthesian coordinates the circular area of subsurface depression with radius d was converted into an equivalent square area of the same volume with half-with $d' = (\sqrt{B} / 2)\,d$. The best fit was achieved for d = 25 m and R = h = 130 m (Fig. 6). The value of S was determined by comparing calculated and measured subsidence in the centre of the profile. A correction was made for the minor "background" subsidence of about 25 mm. S proved to be 1.54 m, which agrees with the seismic data.

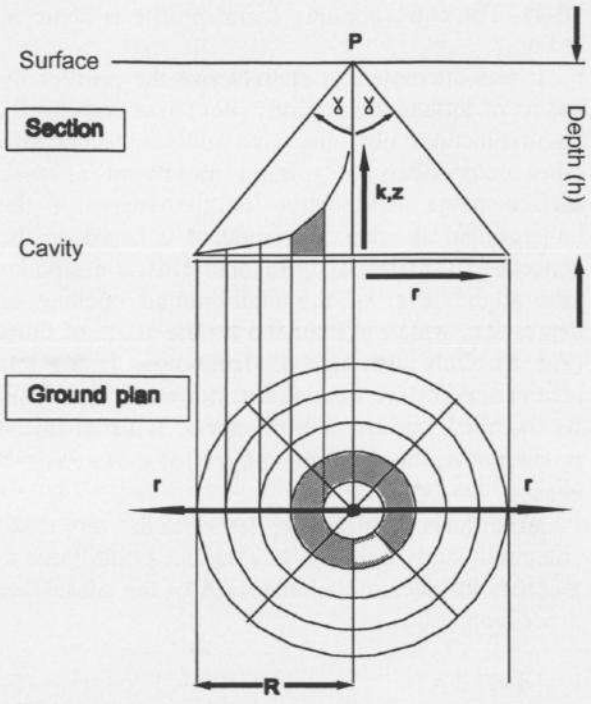

Figure 8. Contribution to surface subsidence at point P by subsurface elements within the radius of influence R.

Tilt v_z' is achieved by taking the first derative of the solution of Eq. 7 and curvature v_z" is equal to the second derative. According to practice [8], horizontal strain ε can be calculated from curvature as follows:

$$\varepsilon = C\,R\,v_z'' \qquad (8)$$

where C is a constant which ranges from 0.05 to 0.5. For all 5 studied subsidence troughs a good fit resulted for C = 0.1 (Fig. 7).

Now the function $F(x,y) = v_z / S$ has been determined. Also the spatial distribution of tilt and horizontal strain in the desired direction are described, by functions $G(x,y) = v_z' / S$ and $H(x,y) = \varepsilon / S$ respectively. While the subsurface depression at wells 30 and 31 is circular, all components of ground movement can also be obtained for elliptical shapes. Then determination of tilt and strain is somewhat more complicated. Depressions of more complex shapes do not need to be considered because of lack of detailed knowledge of their dimensions.

5. GENERAL PREDICTION OF TOTAL SUBSIDENCE

Now S(t) had to be determined using Eq. 3, which describes the relationship between decelerating phase III subsidence and time for point 30-2, and the value of F(x,y) for this point. The first subsidence at this point has developed during phases I and II. The subsidence at the end of phase II and at the onset of acceleration of ground movements is denoted $v_{z,IIIA} = \Delta v_{z,I\text{-}II}$. This subsidence is considered as constant throughout the later to be formed subsidence bowl, because phase I and II subsidence resulted from subsurface events well below the rock-soil boundary. As a consequence, this subsidence was divided over a relatively large horizontal extent. This is rough approximation, but is has to be noted that during phases I and II a relatively minor part of the total subsidence was formed. Then phase III subsidence developed, first during acceleration ($\Delta v_{z,IIIA}$) and then during deceleration ($\Delta v_{z,IIID}$). Accordingly the total subsidence can be divided in three components:

$$v_{z,tot} = \Delta v_{z,I\text{-}II} + \Delta v_{z,IIIA} + \Delta v_{z,IIID} \qquad (9)$$

It has to be noticed that S(t) and F(x,y) apply to the complete phase III, including the accelerating part. Accordingly:

$$F(x,y) * S(t) = \Delta v_{z,IIIA} + \Delta v_{z,IIID} \qquad (10)$$

Combination of Eq. 10 and the regression equation of decelerating phase III for point 30-2, Eq. 3, yields S(t):

$$S(t) = \frac{\Delta v_{z,IIIA} + [-a + b \log \Delta t_{IIID}]_{30-2}}{[F(x,y)]_{30-2}} \qquad (11)$$

Now total subsidence, tilt and strain can be predicted at each arbitrary surface point P according to respectively:

$$[v_{z,tot}]_P =)v_{z,I\text{-}II} + S(t)\,[F(x,y)]_P \qquad (12)$$

$$[v'_{z,tot}]_P = S(t)\,[G(x,y)]_P \qquad (13)$$

$$[\ _{,z,tot}]_P = S(t)\,[H(x,y)]_P \qquad (14)$$

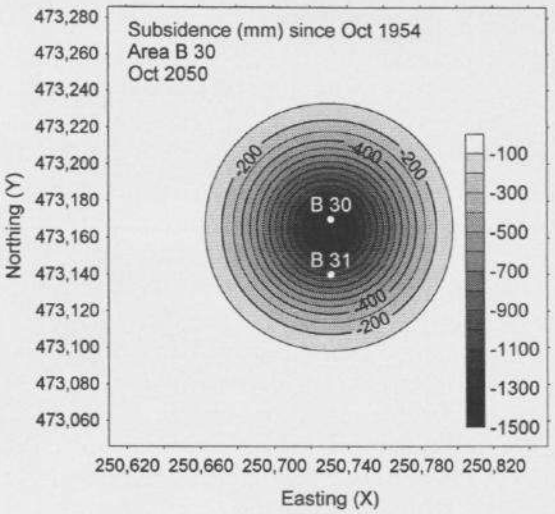

Figure 9. Predicted subsidence at wells 30 and 31.

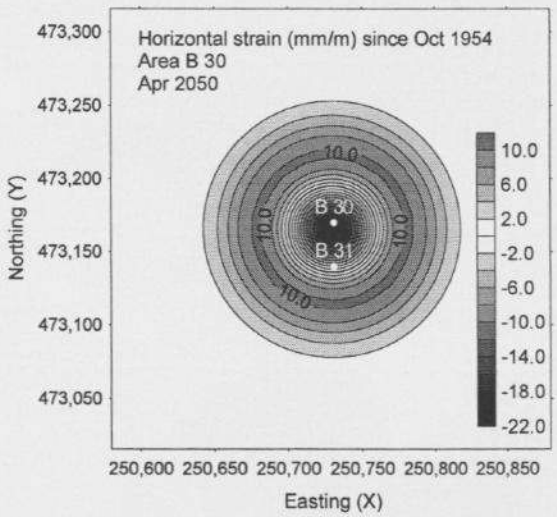

Figure 10. Predicted radial horizontal strain at wells 30 and 31. Positive strain is tensile, negative strain is compressive.

The results of the calculation method are illustrated in Figs. 9-10, which represent surface contour plots of total subsidence and strain towards the centre of the subsidence trough, predicted for 2050 near wells 30 and 31.

CONCLUSIONS

An analysis of the subsidence-time relationship at a given surface point gives an accurate prediction of further trough subsidence over a salt solution cavity, migrated up to the base of a thick soil mass. The same goes for tilt and strain if data from two neighbouring points are involved. Prediction of future ground movement is possible 5 to 10 years after the onset of trough subsidence and applies exclusively to the analysed points. In this analysis S(t), the depth of the subsurface depression at the base of the soil mass as a function of time, and F(x,y), which describes the spatial distribution of subsidence for the whole trough, are not established. F(x,y) is obtained by analysing one or more subsidence profiles and applying a Litwiniszyn-type influence function. By combining these results also S(t) can be determined. Now all components of future ground movement can be predicted for the whole subsidence trough, albeit in less detail than by the analysis for a singular point.

REFERENCES

1. T.H. Wassmann, Mining subsidence in the East Netherlands, Fifth Int.Symp.on Salt,I (1980).
2. R.F. Bekendam, Stoping in weak rock over salt solution cavities in the Hengelo Field, The Netherlands, and its expression in terms of surface subsidence, SMRI Spring Meeting, Cracow, 1-25 (1997).
3. D.M. Cruden, The form of the creep law for rock under uniaxial compression, Int.J.Rock.Mech.Min.Sci., 8, 105-126 (1971).
4. R.F. Bekendam, Pillar stability and large-scale collapse of abandoned limestone room and pillar mines in South-Limburg, The Netherlands, PhD thesis, pp. 361 (1998).
5. T.W. Lambe and R.V. Whitman, Soil Mechanics, John Wiley & Sons, pp. 553 (1979).
6. J. Durbin and G.S. Watson, Testing for serial correlation in least squares regression. II, Biometrika, 38, 159-178 (1951).
7. R.F. Bekendam, Subsidence evaluation over salt solution cavities by means of high resolution 3D seismic reflection in the Hengelo Field, The Netherlands, SMRI Meeting,Rome,23-40 (1998).
8. H. Kratzsch, Mining subsidence engineering (in German), Deutscher Markscheider-Verein, Bochum (1997).